Multi organ assessment of Compensated Cirrhosis Patients using quantitative Magnetic Resonance Imaging

Christopher R Bradley[1,2], Eleanor F Cox[1,2], Robert A Scott[2] ,Martin W James[2], Phillip Kaye[2] Guruprasad P Aithal[2,3], Susan T Francis[1,2]*, Indra Neil Guha[2,3]*

[1] Sir Peter Mansfield Imaging Centre, School of Physics and Astronomy, University of Nottingham, Nottingham, UK

[2] NIHR Biomedical Research Centre, Nottingham University Hospitals NHS Trust and the University of Nottingham, Nottingham, UK

[3]Nottingham Digestive Diseases Centre, School of Medicine, University Of Nottingham, Nottingham, UK

*Joint senior authors

Correspondence:

Dr I. Neil Guha

National Institute for Health Research (NIHR) Nottingham Biomedical Research Centre, Nottingham University Hospitals NHS Trust and University of Nottingham ,

E Floor, West Block QMC, Queens Medical Centre,

Nottingham, NG7 2UH, UK

Phone: +44 (0) 115 8231162

Email: Neil.Guha@nottingham.ac.uk

Keywords: Compensated Cirrhosis, Magnetic Resonance Imaging, Arterial Spin Labelling, Phase Contrast, Longitudinal T1 relaxation time.

Word Count:

Number of Figures and Tables: 8 figures and no tables.

Conflict of interest

None to report

Financial Support

Financial support was received from the NIHR Biomedical Research Centre (NIHR BRC); Gastrointestinal and Liver Disorder theme, Nottingham University Hospitals NHS Trust and University of Nottingham. This article presents independent research funded and supported by the NIHR Nottingham Digestive Diseases Biomedical Research Unit, Nottingham University Hospitals NHS Trust and University of Nottingham. Views expressed are those of the authors and not necessarily those of the NHS, NIHR or Department of Health.

Author Contributions CRB (Acquisition, analysis and interpretation of data, statistical analysis, drafting of the manuscript), EFC (Acquisition, analysis and interpretation of data, critical revision of the manuscript), RS and PK (Acquisition of data and criticial revision of the manuscript), MWJ and GPA (critical revision of the manuscript), STF (Study concept and design, acquisition, analysis, interpretation of data, statistical analysis, drafting of the manuscript), and ING (Study concept and design, interpretation of data, statistical analysis, drafting of the manuscript).

Abstract

Background and Aims: Advancing liver disease results in deleterious changes in a number of critical organs. The ability to measure structure, blood flow and tissue perfusion within multiple organs in a single scan has implications for determining the balance of benefit versus harm for therapies. Our aim was to establish the feasibility of Magnetic Resonance Imaging to assess changes in compensated cirrhosis (CC), and relate this to disease severity and future liver related outcomes (LROs).

Methods: 60 CC patients, 40 healthy volunteers and 7 decompensated cirrhotics were recruited. In a single scan session, MRI measures comprised phase-contrast MRI vessel blood flow, arterial spin labelling tissue perfusion, T_1 longitudinal relaxation time and volume assessment of liver, spleen and kidneys, heart rate and cardiac index. We explore MRI parameters with disease severity and differences in baseline MRI parameters in those 11 (18%) of CC patients who had future LROs.

Results: In the liver compositional changes were reflected by increased T_1 in progressive disease ($p<0.001$) and an increase in liver volume in CC ($p=0.006$), with associated progressive reduction in liver ($p < 0.001$) and splenic ($p<0.001$) perfusion. A significant reduction in renal cortex T_1 and increase in cardiac index and superior mesenteric arterial (SMA) blood flow was seen with increasing disease severity. Baseline liver T_1 ($p=0.01$) and perfusion ($p< 0.01$), and renal cortex T_1 ($p<0.01$) were significantly different in CC patients who subsequently developed negative LROs.

Conclusions: MRI allows the contemporaneous assessment of organs in liver cirrhosis in a single scan without the requirement of contrast agent. MRI parameters of liver T_1, renal T_1, hepatic and splenic perfusion, and SMA blood flow were related to risk of LROs.

Lay Summary

This study assesses the changes to structure, blood flow and perfusion that occur in the key organs (liver, spleen and kidney) associated with severe liver disease (compensated cirrhosis). Those MRI measures which change with disease severity and are related to negative liver related clinical outcomes are described.

Graphical Abstract

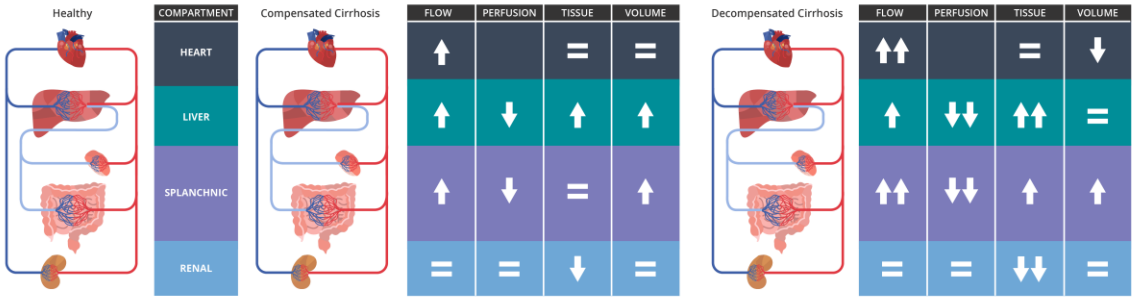

Highlights

- Assessment of MRI parameters in a single scan session.
- Higher liver T_1 and reduced liver perfusion with increasing disease severity and clinical outcomes.
- Reduced renal cortex T_1 linked to disease severity and clinical outcomes.

Introduction

The evolution of liver cirrhosis to clinical liver related outcomes resulting from portal hypertension is not simply dictated by architectural and haemodynamic changes within the liver. Rather, advancing liver disease results in deleterious changes in a number of critical organs and the understanding of this process is a central aspect in the clinical management of cirrhotic patients.

The hyperdynamic circulation in cirrhosis is characterised by increased cardiac output and decreased systemic vascular resistance with low arterial blood pressure [1-3]. Splanchnic vasodilation, with a resulting decrease in the effective central volume, has been proposed as an important driver of the hyperdynamic circulation [1, 4]. Associated with splanchnic vasodilation is an increase in portal vein blood flow which maintains and perpetuates portal hypertension [5]. Further, architectural and haemodynamic changes in the heart, spleen, and kidney have also been shown to occur and have important pathophysiological consequences. For example, cirrhotic cardiomyopathy is characterised by increased cardiac output with a sub-optimal ventricular response to stress, and structural and electrophysiological abnormalities [2]. Cardiac dysfunction associated with cirrhosis has been shown to be an important prognostic determinant of mortality at 1 year [6]. Renal vasoconstriction, related to splanchnic vasolidation, portal hypertension and activation of compensatory neurohormonal systems, is a precursor for the development of hepatorenal syndrome [3, 6, 7]. In cirrhosis, splenic enlargement may result from portal venous congestions and/or hyperplasia. In association, the splenic artery is suggested to dilate [8], and recent data suggests that the splenic artery to hepatic artery diameter ratio can predict the development of ascites and varices [9]. Splenic stiffness has been found to have a strong association with

portal hypertension [10, 11]. However, we have an incomplete understanding of how changes in the different organs are inter-related and their temporal relationship.

The importance of assessing critical organs in liver cirrhosis in a holistic fashion is illustrated by the current controversy surrounding beta-blockers in liver cirrhosis. The debate regarding the safety of beta-blockers focuses on whether the beneficial effects of beta-blockers in liver cirrhosis, centred around a reduction in cardiac output, splanchnic vasodilation and portal inflow and improvement in intrahepatic resistance (alpha 1 blockade), is counterbalanced by deleterious effects in advanced cirrhosis centred on a reduction in renal perfusion and cardiac output as described previously [12]. A key limitation in being able to define the critical window [6, 13] of benefit of beta-blockers versus harm is the lack of robust non-invasive tools to measure changes across organs in a contemporaneous manner. If this could be done, treatment could be indiviudalised more effectively. This does not currently occur in clinical practice, in a consistent manner, as the tools for measurement are blunt (e.g. heart rate) or invasive (hepatic venous pressure gradient measurement (HVPG)).

Recent advances in non-invasive magnetic resonance imaging (MRI) techniques allow the assessment of blood flow to organs [14], tissue perfusion [15, 16], and compositional changes including fibrosis and inflammation, [17-19], in the key organs associated with cirrhosis. Until now, such measures have only been examined in single organs rather than using a comprehensive multi-organ approach in a single scan session.

Our aim was to assess the feasibility of performing MRI in contemporaneous organs of the liver, heart, spleen and kidneys in patients with compensated cirrhosis. We aim to describe the differences in quantitative MRI measures within these organs between healthy volunteers, and patients with compensated cirrhosis and decompensated cirrhosis. As proof

of concept, we explore whether differences in MRI parameters are observed in patients with future clinical liver related outcomes.

Materials and Methods

Study Population

Sixty patients were consecutively recruited from a compensated cirrhosis (CC) cohort study, a prospective study initiated in 2010 focussed on tracking liver disease progression. Here, baseline measures collected for this cohort are reported. Institutional and local research approval was gained (10/H0403/10). Patients were recruited with evidence of cirrhosis (confirmed by a combination of biopsy, clinical and radiological criteria) and no evidence of decompensation (ascites, significant jaundice, hepatic encephalopathy and variceal bleeding), hepatocellular carcinoma and portal vein thrombosis. Exclusion criteria included orthotopic liver transplantion, ischaemic heart disease, alcoholic cardiomyopathy (defined by clinical evidence of systolic dysfunction) and valvular heart disease.

For comparator measures, we prospectively recruited two additional groups – healthy volunteers and decompensated cirrhotics. Fourty healthy volunteers were recruited who had no major co-morbidty including cardiovascular or chronic liver disease. Seven ambulatory, decompensated cirrhosis patients were recruited, defined as Baveno 3 or 4 stage (ascites, encephalopathy or previous variceal bleed); exclusion criteria included portal vein thrombosis, the presence of hepatocellular carcinoma (HCC), and orthotopic liver transplantation . Subjects attended on a single study day following an overnight fast. Statistical power to assess the difference between groups was determined for each MRI parameter at a power of 80 % and significance level of 5 %.

Patients were invited back for research visits on a six monthly basis to assess for a liver related clinical outcome as defined by ascites (needing paracentesis or diuretic therapy), grade 3 or grade 4 encephalopathy, variceal haemorrhage requiring endoscopic therapy and emergency admission, HCC (as defined by EASL criteria) and liver related death. For patients who declined follow up visits, we obtained their consent to access relevant medical records (both family practitioner and hospital records) to record clinical outcomes.

Multiorgan MRI Protocol

All participants were scanned following a 6-hour fast, with MRI scans carried out between 8am-12pm. Imaging was performed on a 1.5 T Philips Achieva MRI scanner (Best, Netherlands) using a 16-element Torso receive coil and body transmit coil. MR measures were collected on four organs: liver – blood flow in the portal vein (PV) and hepatic artery, liver perfusion and tissue T_1; spleen and superior mesenteric artery (SMA) - blood flow assessed in the splenic and SMA, splenic tissue perfusion and tissue T_1; renal – blood flow in right renal artery, kidney volume, renal tissue perfusion and tissue T_1; heart - aortic blood flow corrected for body surface area (BSA) to yield cardiac index and left ventricular (LV) wall mass as a measure of cardiac strain. This non-invasive protocol took less than one hour for hepatic (~ 20 minutes), spleen, SMA and renal (~ 15 minutes), and cardiac (~ 10 minutes) measures. The following describes the acquisition protocol parameters.

Organ volume: First multi-slice balanced turbo field echo (bTFE) localiser images were acquired in three perpendicular orientations to locate organs and vessels of interest for slice positioning, and from which to estimate organ (liver, kidney and spleen) volume.

Blood Flow measures: Phase contrast (PC)-MRI was used to quantify vessel lumen cross-sectional area (CSA), velocity and bulk blood flow in vessels within each system. A TFE technique (2 averages, TFE factor 4–6 dependent on subjects' heart rate) was used with a single slice perpendicular to the vessel of interest. 15 phases were collected across the cardiac cycle using specified velocity encoding for each vessel (portal vein 50cm/s, hepatic/splenic/renal arteries 100cm/s, superior mesenteric artery 140cm/s). Each vessel measurement was acquired during a 15-20s breath hold.

Perfusion of the liver, spleen and kidney: Respiratory-triggered flow alternating inversion recovery arterial spin labelling (FAIR-ASL) [15, 16](post-labelling delay 1100ms, balanced fast field echo (bFFE) readout) was used to measure tissue perfusion in the liver, spleen and renal tissue. Liver perfusion data was acquired in 3 sagittal slices through the right lobe (slice gap 5 mm, 60 ASL pairs in ~ 8 minutes), spleen/renal perfusion data was collected in 5 contiguous coronal-oblique slices through the spleen and long axis of the kidney (30 ASL pairs in ~ 5minutes). An equilibrium base magnetisation M_0 and T_1 image was acquired for each slice orientation for perfusion quantification.

Relaxometry of the liver, spleen and kidney: A modified respiratory-triggered inversion-recovery sequence [16, 19, 20] was used to measure tissue T_1 in the liver, spleen and kidney, with slices geometrically matched to the ASL data. For liver tissue, a fat suppressed spin-echo echo planar imaging (SE-EPI) readout was used to ensure no influence of fat on T_1 measures. Data was collected at 13 inversion times (TI) (100-1200 ms in 100 ms steps, and 1500 ms) with minimal temporal slice spacing between the three slices (65 ms) collected in a descend slice order, in an acquisition time of ~ 2 minutes. For the spleen and kidney, a bFFE readout was used and data acquired at 9 TIs (100-900 ms in 100 ms steps) with minimal temporal slice

spacing (144 ms), both ascend and descend slice order acquisitions were acquired to increase the dynamic range of inversion times [16, 19, 20] in ~ 3 minutes. Subjects were confirmed to not have excess iron [16, 19, 20].

Cardiac assessment: Cardiac output was measured using a PC-MRI of the aorta with 30 phases and velocity encoding of 200 cm/s in ~ 1 minute whilst free breathing. Short-axis cine images were acquired to measure LV wall mass using a multi-slice TFE sequence (12 slices, 30 phases, 3 slices acquired per 15-20 s breath hold).

Data Analysis

Blood Flow Measures: 'Q-flow' software (Philips Medical Systems) was used to analyse PC-MRI data. For each vessel, a region-of-interest (ROI) was drawn to estimate flow by averaging the flow velocity values within the ROI and multiplying by vessel lumen CSA. Mean flow was calculated by averaging the flow rates for each cardiac phase across the cardiac cycle.

Perfusion: Supplementary Figure 1 shows the analysis procedure for ASL data performed using MATLAB and/or IDL routines. Each ASL label/control image was motion corrected to the base magnetisation M_0 image using in-house software. Individual perfusion weighted images (control-label) were calculated, inspected for motion (exclude>1 voxel movement) and averaged to create a single perfusion-weighted image (ΔM). ΔM, M_0 and T_1 maps were used in a kinetic model [21] to compute tissue perfusion maps. A binary mask of each organ (see *Relaxometry* section) was formed and used to calculate the mean liver, spleen and renal cortex perfusion.

Relaxometry: Inversion recovery data were fit to a 2-parameter model to generate T_1 and M_0 maps. Binary organ masks were formed from the M_0 image, and major blood vessels further segmented by excluding voxels with a $T_1 > 1500$ ms. Median T_1 values were calculated within

liver and spleen masks. For the kidney mask, a histogram of T_1 values was formed to yield two peaks originating from the renal cortex and medulla (Supplementary Fig. 1a), and the median T_1 values of the renal cortex and medulla calculated.

Volume: Analyze® (Mayo Clinic) was used to draw an ROI around each organ (liver, kidney, spleen) within each slice, and total organ volume calculated by summing across slices.

Cardiac: Cardiac MRI data was analyzed using ViewForum software (Philips Medical Systems, Best, Netherlands). PC-MRI data of the aorta was analyzed by computing the stroke volume and heart rate, and multiplying these parameters to yield cardiac output. This software was also used to draw wall contours from which LV wall mass was calculated. Both cardiac output and LV wall mass are presented corrected for BSA [22].

Validation of MR measures

T_1 Relaxometry of the Liver: We assessed liver histology in a cohort of cirrhosis patients who previously had T_1 mapping of the liver on a 1.5 T scan [19, 20], all MRI scans were collected within 3 months of liver biopsy. Liver biopsies were obtained via eith er the percutaneous or the transjugular route from patients with METAVIR fibrosis stage 4. Patients were fasted overnight before the procedure and biopsies were carried out by experienced operators. Biopsies were stained with hematoxylin and eosin, picrosirius red (PSR) and Perls' Prussian blue stains. All biopsy data were analysed by a single experienced pathologist blinded to MRI data. The percentage of fibrous tissue relative to the total biopsy area was estimated for each biopsy by visual morphometry [17]. A Spearman's rank correlation coefficient (in terms of R value) was computed between the continuous variables of visual morphometry and liver tissue T_1.

All CC patients had a blood sample to assess non-invasive markers of liver fibrosis (ELF (enhanced liver fibrosis) score). In addition, in all CC patients transient elastography evaluation was performed using FibroScan® (EchoSens, Paris, France) to provide a liver stiffness measure (LSM) in kPa. The Fibroscan® measure was repeated to obtain 10 readings and a median LSM value calculated. Spearman's rank correlation coefficients (R value) are presented between ELF and LSM with a statistical significance threshold of $p < 0.05$.

ASL Perfusion of the Liver: In all patients, measures of Indocyanine green (ICG) were performed and plasma disappearance rate (ICG-PDR, percentage of ICG eliminated in 1 minute after an ICG bolus) (%/min), and its retention rate at 15 minutes (ICGR15, the circulatory retention of ICG during the first 15 minutes after a bolus injection (%)) computed. A Spearman's rank correlation coefficient was performed beyween ICG-PDR and ICGR15 and liver perfusion as measured using arterial spin labelling. Correlation coefficients are presented in terms of R value with a statistical significance threshold of $p < 0.05$.

Repeatability of Multiparametric MRI Measures: To determine the between session repeatability of MRI measures, the intra-subject Coefficient of Variation (CoV) (defined as the standard deviation/mean) of multiparametric MRI measures were assessed. A subset of 10 healthy participants (age 23-37 years, body mass index 20-26 kg/m^2) had three scans, at least one week apart and within four weeks, at the same time of day and after an overnight fast to limit diurnal and dietary variability. Supplementary Table 1 provides the CoV measures.

Statistical Analysis

All statistical analysis was performed using Prism 6 (GraphPad Software, Inc., La Jolla, CA). A Shapiro-Wilk normality test was applied to data collected on each MRI parameter. Normal data is expressed as mean (SEM) and non-normal as median (interquartile range, IQR) across each group. Tests between the three patient groups were made using a one-way analysis of variance (One-Way ANOVA) with Bonferroni correction for normally distributed data, else a Kruskal-Wallis test was performed to assess probable differences between the groups, with post-hoc Tukey's test where significant differences were identified.

To compare results between CC patients without and those with a negative liver related clinical outcome, a two-tailed unpaired t-test was performed to assess differences in normally distributed parameters, else a Mann-Whitney U test was performed, significance was considered at $p < 0.05$. In addition, to test the probability of organ involvement in outcome, a survival analysis was performed providing Kaplan–Meier curves and significance of difference determined by log-rank test, using the 1^{st} tertile of MRI parameters as cut-off values.

Results

The CC cohort (n=60) comprised 25 females (F)/35 males (M) of 60 ± 9 years with a range of aetiologies, the largest being Alcoholic Liver Disease (ALD, 21 patients, 35%), Non-Alcoholic Fatty Liver Disease (NAFLD, 16 patients, 27%), and Hepatitis-C Virus (HCV, 12 patients, 20%), with the remaining 18% of patients having primary biliary cirrhosis, hepatitis B virus, primary sclerosing cholangitis, autoimmune hepatitis and haemochromatosis. Mean MELD, Fib4 and Apri scores were 7.7±2.1, 3.4±2.3, and 1.2±1.2. Of this group, 6 patients were on beta-blockers. The healthy volunteer (HV) group (n=40) comprised 17F/23M subjects of 59±10 years. The decompensated cirrhosis (n=7) (DC) group comprised 5F/2M patients of 48±13

years, with 5 ALD, 1 NAFLD and 1 HCV and decompensation type being 4 ascites, 2 varices and 1 encephalopathy. Mean MELD, Fib4 and Apri scores were 9.9±3.3, 3.5±1.6, and 1.4±1.1.

Validation of MR measures

T_1 Relaxometry of the Liver: T_1 relaxation time correlated significantly with visual morphometry of percentage fibrosis in advanced F4 fibrosis (R=0.62, p<0.001), Supplementary Figure 2. As a secondary outcome, we show a significant positive correlation of liver tissue T_1 with ELF score, R=0.65 and p< 0.001, Supplementary Figure 3. In addition, a highly significant correlation of liver tissue T_1 with the LSM from Fibroscan® was demonstrated (R=0.68, p< 0.001), Supplementary Figure 3.

ASL Perfusion of the Liver: In all patients ICG measures were collected and correlated with liver perfusion as measured by ASL. A weak but significant positive correlation was demonstrated between liver perfusion measured using ASL and ICG-PDR (R=0.46, p=0.0016), and negative correlation with ICGR15 (R=0.46, p=0.0011), Supplementary Figure 4.

Repeatability of Multiparametric MRI Measures: Intra-subject repeatability for all the multiparametric MRI measures is provided in Supplementary Table 1. Measurement of MR parameters is highly repeatable with a CoV of <10 % in assessment of volume, T_1 relaxometry measures, and ASL perfusion.

Changes in Compensated and Decompensated Cirrhosis compared to Healthy Volunteers

In the following section, MRI measures are provided for each organ studied – liver, spleen and SMA, renal and cardiac - and compared across stage of disease severity i.e. HV vs CC vs DC.

Liver: Figure 1 shows the changes measured in the liver across the three groups. Liver volume was significantly greater in CC patients compared to both HVs and DC patients (p=0.006). We observed liver tissue T_1 progressively increased with disease severity, from HV to CC and DC (p<0.001), with statistically significant differences between HV and CC (p<0.001), and the CC and DC groups (p=0.01). Portal vein CSA significantly increased in CC compared to HVs (p<0.001). The cross sectional area of the hepatic artery (HA) increased with disease severity (though not significant p=0.09). Total hepatic blood flow (PV+HA flow) significantly increased with disease severity (p = 0.03). The percentage contribution of PV flow to total hepatic flow (PV flow + HA flow) did not significantly change with liver disease severity (77.9±1.2%, 72.8±1.9%, and 74.5±6.7% for HV, CC, and DC respectively). Liver perfusion significantly reduced with disease severity (p<0.001), with statistically significant differences between HV and CC (p<0.001), and the CC and DC groups (p<0.01).

Spleen and superior mesenteric artery: Figure 2 shows changes in the spleen and SMA across the groups. Spleen volume increased in CC and DC compared to HVs (p<0.03; 206±16ml, 459±34ml, and 490±112ml for HV, CC, and DC respectively), with spleen T_1 increasing with disease severity. No significant difference was found in CSA of the splenic artery, whilst splenic artery bulk flow significantly increased with disease severity (p<0.001). Superior mesenteric artery bulk flow showed an increasing with disease severity. Spleen tissue perfusion significantly decreased with disease severity (p<0.001, 151±7ml/100g/min, 120±6ml/100g/min, and 82±9ml/100g/min for HV, CC, and DC respectively).

Renal: Figure 3 shows changes across the groups. No significant difference is seen in total renal volume between the HV, CC and DC groups. A significant reduction in renal cortex T_1 (p< 0.001) was demonstrated with disease severity, a trend for reduced T_1 was found in the renal

medulla but this was not significant. No significant difference was found in CSA of the renal artery or renal artery bulk flow, but flow per beatreduced with disease severity. No significant difference in renal cortex perfusion was found between the HV, CC, and DC groups.

Cardiac: Figure 4 shows cardiac parameters across the groups. Cardiac index significantly increased with disease severity ($p=0.005$). This was driven by the increase in heart rate with disease severity ($p<0.001$, 59.6±1.6, 67.2±1.6, 76.2±3.1 beats per minute (bpm) for HV, CC, and DC respectively), no significant change in stroke volume was found with disease severity. BSA corrected cardiac LV wall mass was significantly differet across the groups ($p=0.02$; 39.0±1.1, 34.0±1.7, 22.3±2.4 g/m^2 for HV, CC, and DC respectively).

Assessment of baseline MR parameters related to a future clinical outcome in patients with compensated cirrhosis at baseline

Here, we present baseline MRI data for those compensated cirrhosis patients who developed a liver related outcome. Of the 60 patients with compensated cirrhosis at baseline (mean MELD score 7.7), 11 patients (18%) developed a future liver related outcome. The median number of days from MRI scan to a liver related outcome was 1001 (range: 59-2304). 7 had ascites, 1 developed encephalopathy, 1 developed a variceal bleed, 2 had hepatocellular carcinoma (HCC). Of these 11 patients, 7 patients died of a liver related cause after the first liver related outcome; liver failure (4 cases) and HCC (3 cases) as listed on the death certificate.

The patients with an outcome were of 59±6 years, 6M/5F, and aetiology comprising 4 HCV, 5 ALD, 1 NAFLD, and 1 HBV. Figure 5 shows how those MR parameters found to have a significant difference between HV, CC and DC patients relate to clinical liver related outcomes.

There was no significant difference in liver volume between CC patients with and without a LRO. In contrast, liver tissue T_1 was significantly higher (p=0.01) in those CC patients with a clinical outcome (834±36ms) compared to those without (719±10ms). The CSA of the portal vein was not significantly different between CC patients with and without a clinical outcome. Total hepatic blood flow was significantly (p=0.05) lower in those with outcomes (13.4±7.6ml/s) compared to those patients with no outcomes (17.8±6.0ml/s). Perfusion measured in the right lobe of the liver was significantly lower (p<0.01) in those patients with an outcome (clinical LRO: 95.8±9.5ml/100g/min, no LRO: 160±8.0ml/100g/min). No significant difference was found in spleen volume or splenic T_1 between those CC patients with and without outcomes, but splenic perfusion was lower and SMA blood flow higher. Renal cortex T_1 was significantly shorter in those CC patients with an outcome (919±28ms) compared to those with no outcome (1012±11ms). There was no significant difference in cardiac measures of cardiac index or LV wall mass index between those CC patients with and without a clinical outcome. Figure 6 shows the use of tertile cut-off points (as used in [23]) of liver perfusion, liver T_1 and renal T_1 used to compute Kaplan-Meier survival curves. These MRI parameters were significant predictors of liver related outcomes.

Discussion

We have shown that it is feasible to study changes in cirrhosis representing the flow, volume, composition and perfusion in critical organs (liver, kidney, spleen and heart) in a contemporaneous fashion in a single scan session using quantitative MRI without the requirement of injection of a contrast agent. Individual MR components change with disease severity, as illustrated by Figure 7, and taken together this data provides a comprehensive evalution of cirrhosis relating to aspects of structure and haemodynamics. Furthermore, a subset of MRI markers measured at baseline (i.e. liver T_1, liver perfusion and renal cortex T_1)

differentiate two groups of CC patients, those who develop or do not develop a future liver related clinical outcome up to 7 years later (Figures 5 and 6).

The study highlights two conceptual aspects that are coherent with our current understanding of how liver disease progresses. Firstly, structural changes as evidenced by changes in organ volume (i.e. spleen and liver) and compositional change (i.e. increased liver T_1 and splenic T_1) relate to increasing disease progression from the spectrum of healthy volunteers to decompensated cirrhosis. Secondly, how changes in haemodynamics both to and within the organ evolve with progressive disease. This is exemplified by the reduction in both liver and splenic perfusion. Despite the small size of the DC group, it is interesting to note that the reduction of hepatic perfusion occurs in the context of increased total hepatic blood delivery in the CC and DC group, though this only results in an increase in normalised hepatic blood flow between the HV and DC group (Supplementary Figure 5). The reduction in liver volume that occurs in decompensated cirrhosis compared to compensated cirrhosis, as previously shown in [24], suggests that this is not related to a larger mass of liver tissue to supply. We hypothesise two explanantions for this discordance. Firstly, intra-hepatic shunting may occur, although using our current MR methods we do not have the spatial resolution to directly visualise shunts. Secondly, in liver disease it is difficult to use normalised hepatic blood flow as a measure of global perfusion due to the underlying changes in liver composition. The deposition of fat, interstitial oedema and inflammatory cells can all potentially increase liver volume. As the liver starts decompensating, these features subside and in addition there is a loss of hepatocyte volume relative to an increasing amount extracellular matrix [25]. This highlights the importance of measuring perfusion rather than blood flow per se.

The increase in splenic artery blood flow is largely compensated for by the increase in spleen volume, with a trend for reduction in normalised splenic flow (Supplementary Figure 5) in agreement with the significant reduction in perfusion. The increase in splenic T_1 also suggests that angio-architectural changes occur within the splee, perhaps related to fibrosis. Finally, there was a trend for reduced renal perfusion, in the context of maintained renal artery bulk flow and increased kidney volume, in agreement with a reduced normalised renal blood flow, Supplementary Figure 5.

Of the 60 compensated cirrhosis patients, six were on beta-blockers with this sub-group showing a significant reduction in splenic artery cross-sectional area, mean velocity and flux, spleen perfusion and portal vein mean velocity, thus increasing the CC cohort group variance in these measures. In addition, the DC sample size is currently underpowered to determine significant incremental changes, except in T_1 relaxometry measures; this remains work in progress.

The significant difference in baseline MRI parameters in those patients at risk of clinical events, within an average follow up period of 3 years and maximium follow up of 7 years, is very encouraging. In this study 18% (11) patients had a negative clinical outcome, this is a similar sample size to a recent study of events using multiparametric MRI of the liver alone and an associated Liver Inflammation and Fibrosis (LIF) score in which 10 patients (11%) were studied [26]. In the current study, we had a higher LRO compared with previous studies (4% in a transient elastography study [27] and 13% in a ELF study [28]). The increased liver T_1 (a marker of structural severity) and reduced liver perfusion (a marker of haemodynamic severity) in patients with early compensated liver cirrhosis achieving future liver related clinical outcomes has biological plausibility and provides a link between surrogate bio-imaging

signals and robust clinical end points. The relevance of the strong relationship of renal cortex T_1 to both disease severity and clinical outcomes is novel. Two studies, in patients with cirrhosis, have suggested changes in T_1 occur within the cortex of the kidney, but until now these studies have been based on signal intensity changes of T_1-weighted images [29, 30], with no quantitative measures of T_1 relaxation times having previously being reported. These previous studies suggest that the mechanism and physiology of reduced renal T_1 is decreased water content in the renal cortex due to renal hypoperfusion. Whilst the overall blood flow to the kidneys was maintained in our study, there was both a trend toward reduced renal perfusion, reduced renal artery flow per beat decreased and kidney volume increased (Figure 3), with a significant reduction in normalised bulk renal blood between healthy volunteers and CC patients (Supplementary Figure 5). Thus it is intriguing to speculate that regional vasoconstriction, driven by neurohormonal mechanisms, accounted for differential water content and reduced T_1. If this is proven to be the case, this has direct implications for the treatment of hepatorenal syndrome.

The overall picture that emerges from this study is consistent with our current understanding of the hyperdynamic circulation and the peripheral arterial vasodilatation hypothesis [4] . With advancing liver disease, reflected by structural changes within the liver (prolonged liver T_1 values, Figure 1) and haemodynamic changes in the liver (reduced liver perfusion, Figure 1), there is a predicted rise in portal pressure (calculated from MRI data as a surrogate measure of HVPG [20] shown in Supplementary Figure 6). Pooling of blood in the splanchnic circulation as evidenced by increased SMA bulk flow and splenic artery bulk flow (Figure 2) perpetuates this raised portal pressure. To accommodate the reduced effective central volume, the cardiac index increases in association with a raised heart rate (Figure 4). Importatly this compensatory mechanism may be fragile as highlighted by the reduced LV

wall mass in decompensated cirrhosis in our study and by others [31]. The decompensated cirrhosis group, albeit small in number, were ambulatory in our study. It is plausible that acute insults, including sepsis, that lead to hospitalisation tip the balance of these compensatory mechanisms. Recently, it has been proposed that vasodilation occurs in a differential manner in regional beds. Using PC-MRI angiography, McAvoy and colleagues [32] found a reduction in total renal blood flow in patients with advanced liver disease compared to healthy volunteers but an increase in total hepatic blood flow and superior mesenteric artery flow. Our data supports this concept of differential visceral blood flow in cirrhosis .

Here we present validation of our MRI measures against the gold standard, showing the correlation of T_1 with the continuous biopsy variable of visual morphometry in METAVIR fibrosis stage F4, in agreement with previous reports in literature across a wider range of fibrosis scores obtained from histology [17, 19]. Further, we show that liver perfusion assessed in this CC cohort shows a significant correlation with Indocyanine green (ICG-PDR and ICGR15). A recent study [33] assessed ICG continuous clearance and HVPG measurement against 2D PC-MRI of portal venous and hepatic arterial flow. They were able to demonstrate useful correlates that suggest benefits further development of MRI protocols for liver blood flow. We acknowledge ICG-PDR and ICGR15 are surrogate and not true measures of perfusion. Formal ICG clearance would be the optimal method, but this requires invasive transjugular hepatic venous sampling and simultaneous peripheral arterial sampling in patients receiving a continuous peripheral ICG infusion, as such this invasive procedure is far less practical. Doppler ultrasound has been widely used to assess blood flow in liver disease [34, 35], and has the advantage of wide availability. However, disadvantages include intra- and inter-observer variation, with reported intra-class variation of 0.49 [36] due to inadequate standardisation of protocols including anatomical site, doppler beam angle and

operator experience. Annet et al. showed PC-MRI parameters have the sensitivity to detect a significant difference between HV and cirrhotics not reflected in doppler ultrasound [34]. Doppler ultrasound has been shown to underestimate blood flow and be less reproducible in comparsion to PC-MRI [37], here we have shown the CoV of PC-MRI to be less than 5% in healthy volunteers [38], further MRI has been shown to be more reliable with respect to inter-observer variability than Duplex Doppler Ultrasound [39]. Several studies have used computed tomography to assess portal vein and hepatic artery blood flow, but this is limited by ionising radiation exposure [40].

This study has a number of clinical implications. Firstly, understanding the benefit versus risk of existing and emerging therapeutics. Betablockers are used as standard care in the setting of portal hypertension. However, non-selective betablockers may be potentially deleterious after a critical threshold or window period has traversed. It remains unclear when that period exactly occurs, but this is likely to be related to diminishing cardiac output and a reduction in renal blood flow [6]. The concept of using MR protocols to assess response to betablockers has been explored by the Edinburugh group. They used PC-MRI to show a significant reduction in cardiac output (as measured by superior aorta blood flow) but maintenance of blood flow in other vessels (SMA, portal vein, hepatic artery, azygous vein) 4 weeks after commencing beta-blocker therapy, though this was in a small cohort of patients who were heart rate responders (n = 9) [13]. Furthermore, using MRI protocols to assess novel drug compounds has been highlighted by the recent report of serelaxin providing therapeutic potential in renal dysfunction in cirrhosis. In this study selective renal vasodilation did not appear to be offset by a reduction in systemic blood pressure or hepatic perfusion [41]. Taken together with our findings, the vision should be to use MRI protocols to assess response at an individual level and thus provide tailored therapy which is effective and safe.

A further application is whether this MRI protocol could serve as a prognostic tool for overall liver outcomes or specific complications. There is a growing body of literature showing the promise of non-invasive markers of liver fibrosis for prognostic performance [42, 43]. The ability of two simple scores Fib4 and APRI to differentiate outcomes in early compensated cirrhosis, as reproduced in this study (Figure 5) cautions against positioning MRI as a generic prognostic tool. However, the difference in parameters between patients with/without significant clinical outcomes is suggestive of the potential to use these parameters for prediction and would be an understandable ambition in the era of emerging anti-fibrotic compounds. Larger studies are required to detemine clinical utility of these promising multiparametric measures related to LROs [44].

This study was designed as a proof of concept study to assess the feasibility of using MRI to assess different organs in cirrhosis and confirms this is possible. Importantly, the scan time for the present protocol is one hour. Whist we have obviated the requirement of intravenous contrast, the scan time can now be reduced by omitting parameters which have been found to be non-contributory. This will be important for patient compliance and reducing cost and burden on radiology service provison time for future implementation into clinical practice. Whilst the MR picture obtained provides an overview it is by no means an exclusive assessment of the hyperdynamic circulation. For example, the current protocol does not provide an assessment of systemic vascular resistance nor does it delineate intrahepatic shunts which we have postulated to underpin the marked reduction in liver perfusion. We deliberately chose aspects of MRI measurements that have been validated previously by our group and others based on comparison to gold standard reference tests including invasive angiography and liver biopsy. The current imaging protocol has been performed on 1.5 T but can easily be applied at 3T, which provides higher signal-to-noise ratio and spatial resolution.

Demonstrating that monitoring of therapy with MRI protocols can change hard clinical outcomes and is cost effective within a multicentred randomised controlled trial will be required before considering implementation into clinical care.

We have shown that quantitative MRI can provide a global picture of cirrhosis by measuring aspects of flow, volume, composition and perfusion in critical organs. The change of key parameters including liver T_1, liver perfusion and renal cortical T_1 in both progressive disease and the differences detected in liver related clinical outcomes has tangible utility in the understanding and treatment of the complications of chronic liver disease.

Acknowledgments

We would like to thank the NIHR Nottingham BRC research nurses, including Antonella Ghezi, Andrea Bennett, Tracey Wildsmith and Louise James who conducted patient enrolment and performed clinical measures, and Rubie-Jo Barker who produced illustrations.

Figure Legends

Fig. 1. Change in the liver in healthy volunteers (HV), compensated cirrhosis patients (CC) and decompensated patients (DC). A) liver volume. B) T_1 within liver tissue. C) Portal vein cross sectional area . D) Portal vein bulk flow. E) Hepatic artery cross sectional area. F) Hepatic artery bulk flow. G) Total hepatic blood flow (portal vein bulk flow + hepatic artery bulk flow). H) Perfusion of liver tissue. Data analyzed using one-way ANOVA, followed by the Tukey *post hoc* test. *p < 0.05, **p < 0.01, ***p < 0.005, ****p < 0.001.

Fig. 2. Changes in the spleen and Superior Mesenteric Artery in healthy volunteers (HV), compensated cirrhosis patients (CC) and decompensated patients (DC). A) Spleen volume. B) Spleen T_1. C) Splenic artery cross sectional area. D) Splenic artery bulk flow. E) Superior mesenteric artery cross sectional area. F) Superior mesenteric artery bulk flow G) Splenic tissue perfusion. Data analyzed using one-way ANOVA, followed by the Tukey *post hoc* test. *p < 0.05, **p < 0.01, ***p < 0.005, ****p < 0.001.

Fig. 3. Changes in the kidney in healthy volunteers (HV), compensated cirrhosis patients (CC) and decompensated patients (DC). A) Total renal volume. B) Renal cortex and medulla T_1. C) Renal artery cross sectional area. D) Renal artery bulk flow. E) Renal artery flow per beat. F) Renal cortex perfusion. Data analyzed using one-way ANOVA, followed by the Tukey *post hoc* test. *p < 0.05, **p < 0.01, ***p < 0.005, ****p < 0.001.

Fig. 4. Changes in the cardiac function between healthy volunteers (HV), compensated cirrhosis patients (CC) and decompensated patients (DC). A) Cardiac Index. B) Body surface area corrected left ventricular wall mass C) Heart rate. Data analyzed using one-way ANOVA, followed by the Tukey *post hoc* test. *p < 0.05, **p < 0.01, ***p < 0.005, ****p < 0.001.

Fig. 5. Baseline MRI parameters in CC patients with and without liver related outcomes. Liver: A) Hepatic volume. B) Portal vein blood flow. C) Total hepatic blood flow. D) Liver perfusion. E) Liver T_1; Spleen and SMA: A) Splenic volume. B) Splenic artery bulk flow. C) SMA bulk flow. D) Splenic perfusion. E) Spleen T_1; Renal/Cardiac: A) Renal cortex T_1. B) Cardiac Index. C) Left ventricular wall mass index; Clinical measures: A) MELD. B) Apri. C) Fib4.

Fig. 6 Kaplan–Meier curves for liver related outcome survival in compensated cirrhosis with patients stratified according to A) Liver T_1 B) Liver perfusion and C) Renal cortex T_1. A) There were significant differences between those with Liver T_1 for the 1st tertile T_1 of 793 ms ($p < 0.001$). B) There was significance between liver perfusion using the 1st tertile of 125 ml/100g/min ($p < 0.001$). C) There was a significant difference between renal T_1 using a 1st tertile of 958 ms ($p < 0.001$).

Fig. 7. Multiorgan changes demonstrated in this study in compensated and decompensated liver disease.

Infographic to pictorially illustrate the changes in key organs (heart, liver, splanchnic and kidney) demonstrated in this study of contemporaneous MR measures in compensated and

decompensated cirrhosis. A hyperdynamic circulation results in increased blood flow in the liver, splanchnic circulation and increased cardiac output in CC patients, with further increases in spleen blood flow and cardiac index in DC patients. Here liver and splenic perfusion was shown to be reduced in CC patients compared to the HV group, and perfusion in these organs is further reduced in DC patients. No significant change in renal perfusion was found between CC and DC patients and the HV group. Tissue demonstrated an increase in T_1 in the liver in CC patients which further increased in DC patients, spleen T_1 was only significantly different from the HV group in DC patients. In contrast renal T_1 was reduced in CC patients and further reduced in DC patients compared to HVs. Left ventricular wall mass significantly reduced in DC patients compared to HVs, whilst liver volume was found to increase only in CC patients, and spleen volume was increased in both CC and DC patients compared to HVs.

References

1. Iwakiri, Y. and R.J. Groszmann, *The hyperdynamic circulation of chronic liver diseases: from the patient to the molecule.* Hepatology, 2006. **43**(2 Suppl 1): p. S121-31.
2. Møller, S. and J.H. Henriksen, *Cardiovascular complications of cirrhosis.* Gut, 2008. **57**(2): p. 268-278.
3. Schrier, R.W., et al., *Peripheral arterial vasodilation hypothesis: a proposal for the initiation of renal sodium and water retention in cirrhosis.* Hepatology, 1988. **8**(5): p. 1151-7.
4. Moller, S. and F. Bendtsen, *The pathophysiology of arterial vasodilatation and hyperdynamic circulation in cirrhosis.* Liver Int, 2018. **38**(4): p. 570-580.
5. Taylor, C.R. and T.R. McCauley, *Magnetic resonance imaging in the evaluation of the portal venous system.* J Clin Gastroenterol, 1992. **14**(3): p. 268-73.
6. Krag, A., et al., *Low cardiac output predicts development of hepatorenal syndrome and survival in patients with cirrhosis and ascites.* Gut, 2010. **59**(1): p. 105-10.
7. Lautt, W.W., *Regulatory processes interacting to maintain hepatic blood flow constancy: Vascular compliance, hepatic arterial buffer response, hepatorenal reflex, liver regeneration, escape from vasoconstriction.* Hepatol Res, 2007. **37**(11): p. 891-903.
8. Blendis, L., L. Kreel, and R. Williams, *The coeliac axis and its branches in splenomegaly and liver disease.* Gut, 1969. **10**(2): p. 85-90.
9. Zeng, D.B., et al., *Abnormal splenic artery diameter/hepatic artery diameter ratio in cirrhosis-induced portal hypertension.* World J Gastroenterol, 2013. **19**(8): p. 1292-8.
10. Colecchia, A., et al., *Measurement of spleen stiffness to evaluate portal hypertension and the presence of esophageal varices in patients with HCV-related cirrhosis.* Gastroenterology, 2012. **143**(3): p. 646-654.
11. Takuma, Y., et al., *Measurement of spleen stiffness by acoustic radiation force impulse imaging identifies cirrhotic patients with esophageal varices.* Gastroenterology, 2013. **144**(1): p. 92-101 e2.
12. Reiberger, T. and M. Mandorfer, *Beta adrenergic blockade and decompensated cirrhosis.* J Hepatol, 2017. **66**(4): p. 849-859.
13. McDonald, N., et al., *Assessment of Haemodynamic Response to Nonselective Beta-Blockers in Portal Hypertension by Phase-Contrast Magnetic Resonance Angiography.* Biomed Res Int, 2017. **2017**: p. 9281450.
14. Applegate, G.R., et al., *Blood flow in the portal vein: velocity quantitation with phase-contrast MR angiography.* Radiology, 1993. **187**(1): p. 253-6.
15. Gardener, A.G. and S.T. Francis, *Multislice perfusion of the kidneys using parallel imaging: image acquisition and analysis strategies.* Magn Reson Med, 2010. **63**(6): p. 1627-36.
16. Cox, E.F., et al., *Multiparametric Renal Magnetic Resonance Imaging: Validation, Interventions, and Alterations in Chronic Kidney Disease.* Front Physiol, 2017. **8**: p. 696.

17. Agrawal, S., et al., *Visual morphometry and three non-invasive markers in the evaluation of liver fibrosis in chronic liver disease.* Scand J Gastroenterol, 2017. **52**(1): p. 107-115.

18. Heye, T., et al., *MR relaxometry of the liver: significant elevation of T1 relaxation time in patients with liver cirrhosis.* Eur Radiol, 2012. **22**(6): p. 1224-32.

19. Hoad, C.L., et al., *A study of T(1) relaxation time as a measure of liver fibrosis and the influence of confounding histological factors.* NMR Biomed, 2015. **28**(6): p. 706-14.

20. Palaniyappan, N., et al., *Non-invasive assessment of portal hypertension using quantitative magnetic resonance imaging.* J Hepatol, 2016. **65**(6): p. 1131-1139.

21. Buxton, R.B., et al., *A general kinetic model for quantitative perfusion imaging with arterial spin labeling.* Magn Reson Med, 1998. **40**(3): p. 383-96.

22. Natori, S., et al., *Cardiovascular function in multi-ethnic study of atherosclerosis: normal values by age, sex, and ethnicity.* AJR Am J Roentgenol, 2006. **186**(6 Suppl 2): p. S357-65.

23. Banypersad, S.M., et al., *T1 mapping and survival in systemic light-chain amyloidosis.* Eur Heart J, 2015. **36**(4): p. 244-51.

24. Tong, C., et al., *Assessment of liver volume variation to evaluate liver function.* Front Med, 2012. **6**(4): p. 421-7.

25. Williams, M.J., A.D. Clouston, and S.J. Forbes, *Links between hepatic fibrosis, ductular reaction, and progenitor cell expansion.* Gastroenterology, 2014. **146**(2): p. 349-56.

26. Pavlides, M., et al., *Multiparametric magnetic resonance imaging predicts clinical outcomes in patients with chronic liver disease.* J Hepatol, 2016. **64**(2): p. 308-315.

27. Pang, J.X., et al., *Liver stiffness by transient elastography predicts liver-related complications and mortality in patients with chronic liver disease.* PLoS One, 2014. **9**(4): p. e95776.

28. Parkes, J., et al., *Enhanced liver fibrosis test can predict clinical outcomes in patients with chronic liver disease.* Gut, 2010. **59**(9): p. 1245-51.

29. Lee, K.S., et al., *Corticomedullary differentiation on T1-Weighted MRI: comparison between cirrhotic and noncirrhotic patients.* J Magn Reson Imaging, 2012. **35**(3): p. 644-9.

30. Yamada, F., et al., *Pseudonormal Corticomedullary Differentiation of the Kidney Assessed on T1-weighted Imaging for Chronic Kidney Disease Patients with Cirrhosis.* Magn Reson Med Sci, 2015. **14**(3): p. 165-71.

31. Merli, M., et al., *Survival at 2 years among liver cirrhotic patients is influenced by left atrial volume and left ventricular mass.* Liver Int, 2017. **37**(5): p. 700-706.

32. McAvoy, N.C., *Editorial: increased cardiac output in cirrhosis - non-invasive assessment of regional blood flow by magnetic resonance angiography. Author's reply.* Aliment Pharmacol Ther, 2016. **43**(12): p. 1342-3.

33. Chouhan, M.D., et al., *Caval Subtraction 2D Phase-Contrast MRI to Measure Total Liver and Hepatic Arterial Blood Flow: Proof-of-Principle, Correlation With Portal*

Hypertension Severity and Validation in Patients With Chronic Liver Disease. Invest Radiol, 2017. **52**(3): p. 170-176.

34. Annet, L., et al., *Hepatic flow parameters measured with MR imaging and Doppler US: correlations with degree of cirrhosis and portal hypertension.* Radiology, 2003. **229**(2): p. 409-14.

35. Popov, D., et al., *Doppler parameters of hepatic and renal hemodynamics in patients with liver cirrhosis.* Int J Nephrol, 2012. **2012**: p. 961654.

36. Iwao, T., et al., *Echo-Doppler measurements of portal vein and superior mesenteric artery blood flow in humans: inter- and intra-observer short-term reproducibility.* J Gastroenterol Hepatol, 1996. **11**(1): p. 40-6.

37. Yzet, T., et al., *Hepatic vascular flow measurements by phase contrast MRI and doppler echography: a comparative and reproducibility study.* J Magn Reson Imaging, 2010. **31**(3): p. 579-88.

38. Chowdhury, A.H., et al., *A randomized, controlled, double-blind crossover study on the effects of 2-L infusions of 0.9% saline and plasma-lyte(R) 148 on renal blood flow velocity and renal cortical tissue perfusion in healthy volunteers.* Ann Surg, 2012. **256**(1): p. 18-24.

39. Vermeulen, M.A., et al., *Accurate perioperative flow measurement of the portal vein and hepatic and renal artery: a role for preoperative MRI?* Eur J Radiol, 2012. **81**(9): p. 2042-8.

40. Motosugi, U., et al., *Multi-organ perfusion CT in the abdomen using a 320-detector row CT scanner: Preliminary results of perfusion changes in the liver, spleen, and pancreas of cirrhotic patients.* European Journal of Radiology, 2012. **81**(10): p. 2533-2537.

41. Snowdon, V.K., et al., *Serelaxin as a potential treatment for renal dysfunction in cirrhosis: Preclinical evaluation and results of a randomized phase 2 trial.* Plos Medicine, 2017. **14**(2).

42. Angulo, P., et al., *Simple noninvasive systems predict long-term outcomes of patients with nonalcoholic fatty liver disease.* Gastroenterology, 2013. **145**(4): p. 782-9 e4.

43. Vergniol, J., et al., *Noninvasive tests for fibrosis and liver stiffness predict 5-year outcomes of patients with chronic hepatitis C.* Gastroenterology, 2011. **140**(7): p. 1970-9, 1979 e1-3.

44. Chouhan, M.D., et al., *Multiparametric magnetic resonance imaging to predict clinical outcomes in patients with chronic liver disease: A cautionary note on a promising technique.* J Hepatol, 2017. **66**(2): p. 455-457.

Final Figures

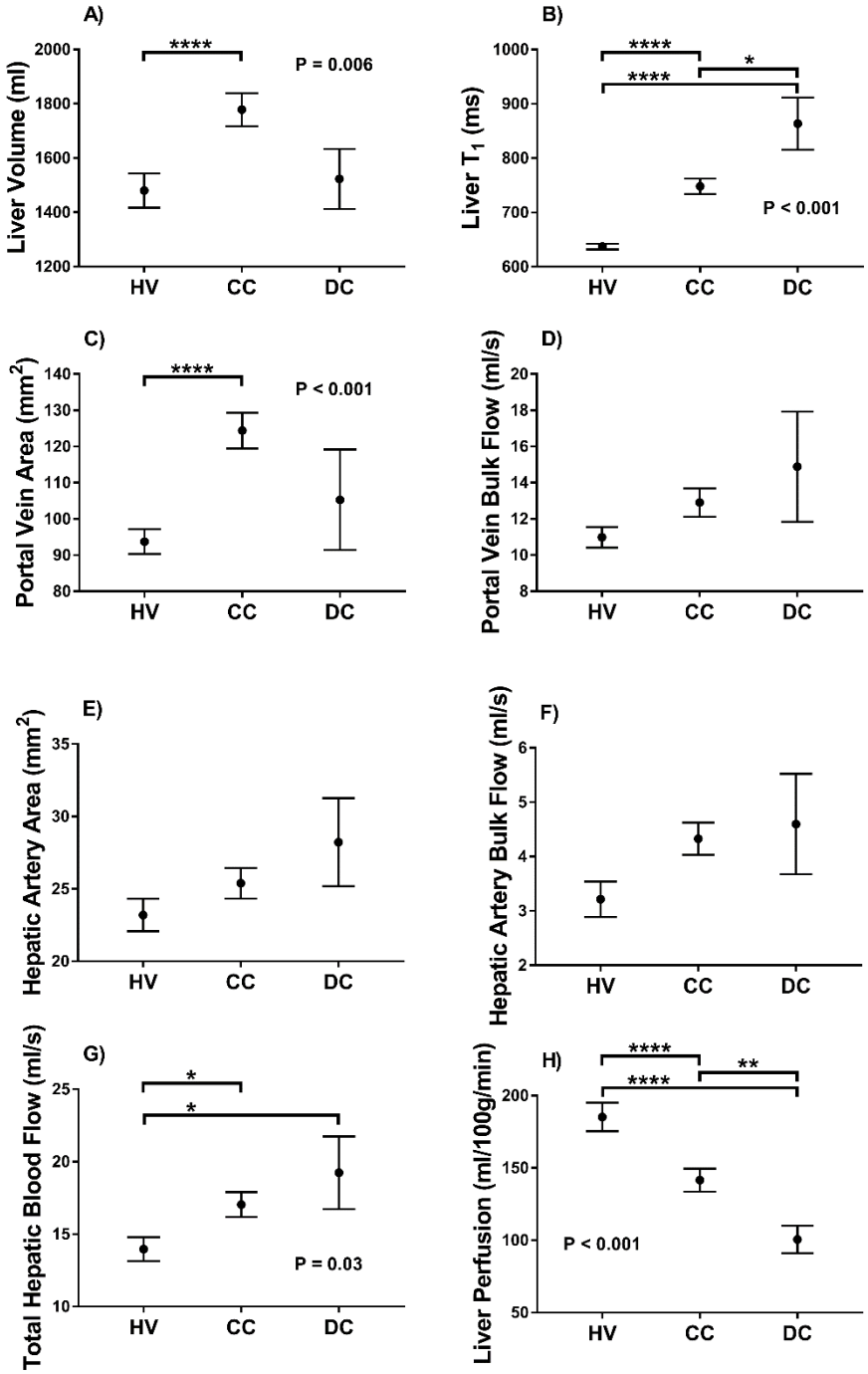

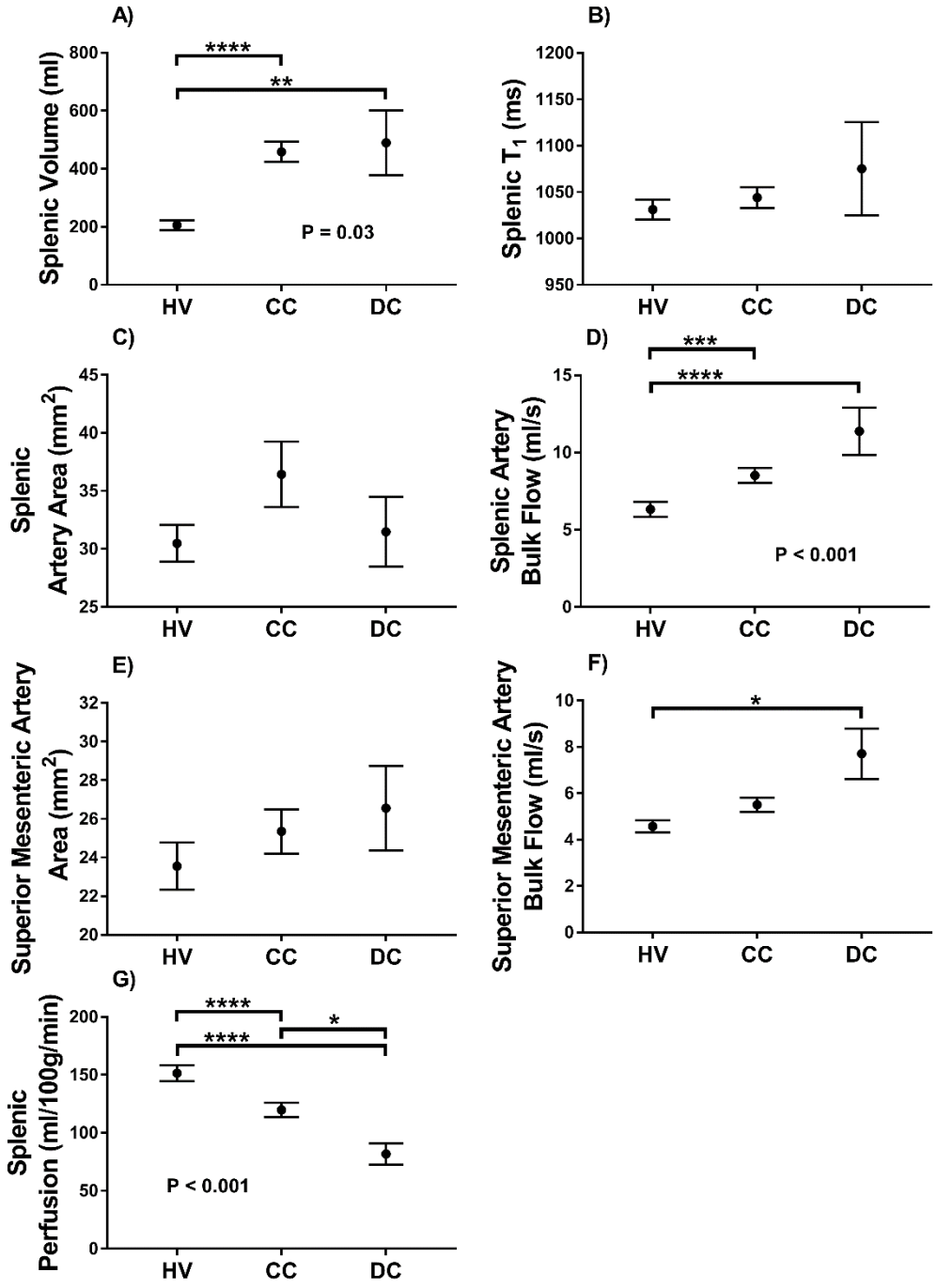
A)
Splenic Volume (ml)
800
600
400
200
0
****
**
P = 0.03
HV
CC
DC
B)
Splenic T_1 (ms)
1200
1150
1100
1050
1000
950
HV
CC
DC
C)
Splenic Artery Area (mm^2)
45
40
35
30
25
HV
CC
DC
D)
***
****
Splenic Artery Bulk Flow (ml/s)
15
10
5
0
P < 0.001
HV
CC
DC
E)
Superior Mesenteric Artery Area (mm^2)
32
30
28
26
24
22
20
HV
CC
DC
F)
*
Superior Mesenteric Artery Bulk Flow (ml/s)
10
8
6
4
2
0
HV
CC
DC
G)
****
*
****
Splenic Perfusion (ml/100g/min)
200
150
100
50
0
P < 0.001
HV
CC
DC

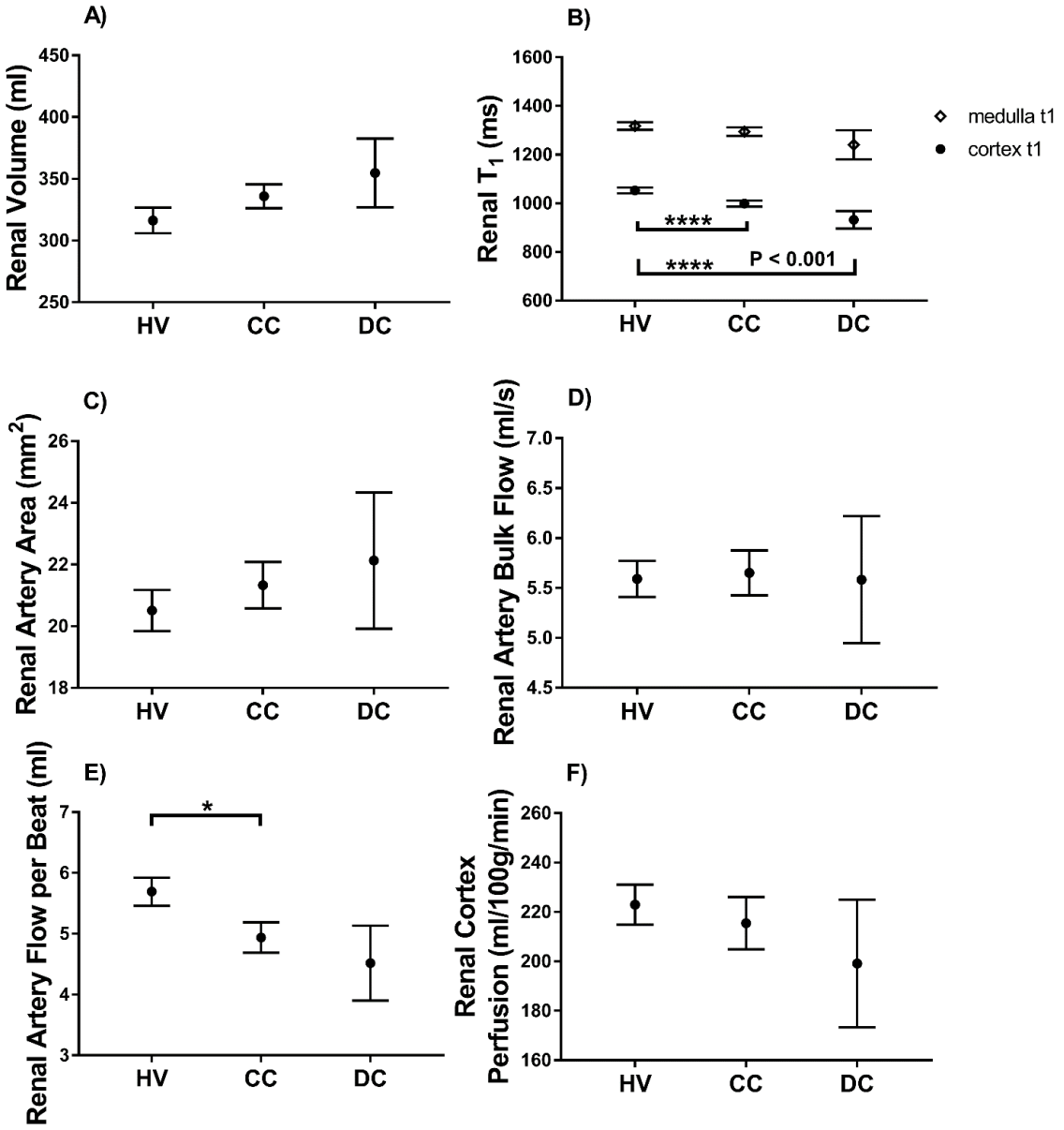
A)
Renal Volume (ml)
450
400
350
300
250
HV
CC
DC
B)
Renal T_1 (ms)
1600
1400
1200
1000
800
600
****
****
P < 0.001
HV
CC
DC
medulla t1
cortex t1
C)
Renal Artery Area (mm^2)
26
24
22
20
18
HV
CC
DC
D)
Renal Artery Bulk Flow (ml/s)
7.0
6.5
6.0
5.5
5.0
4.5
HV
CC
DC
E)
Renal Artery Flow per Beat (ml)
*
7
6
5
4
3
HV
CC
DC
F)
Renal Cortex Perfusion (ml/100g/min)
260
240
220
200
180
160
HV
CC
DC

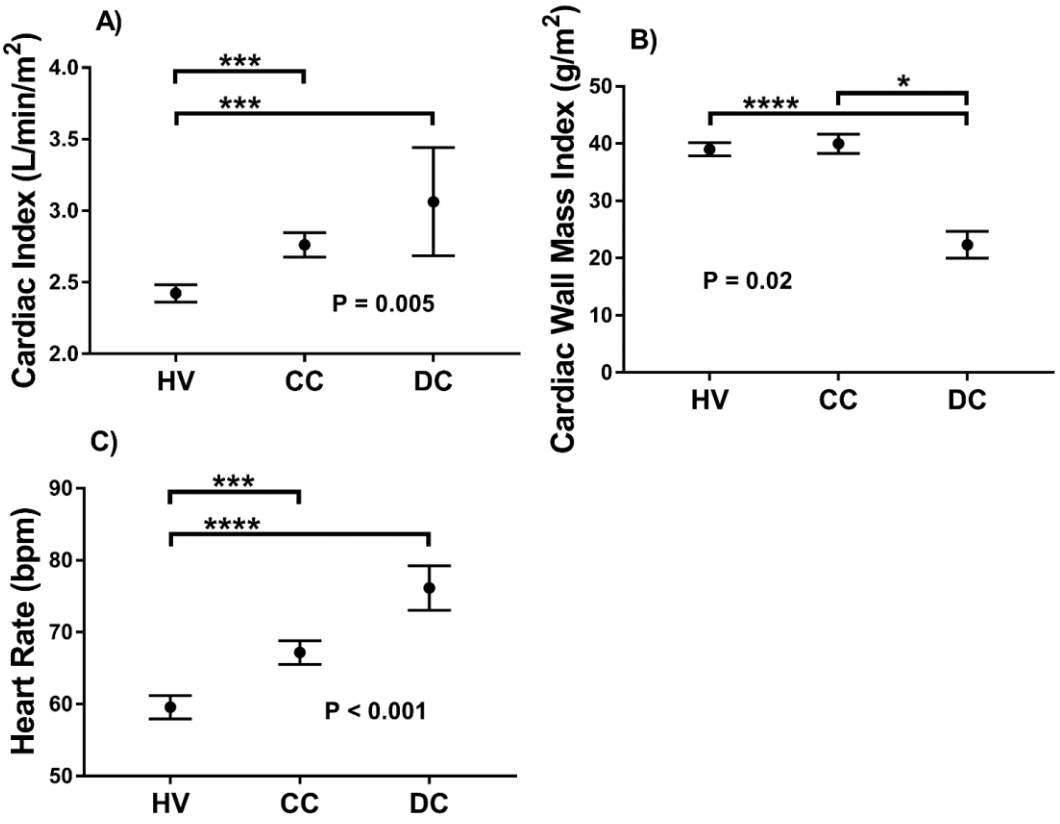
A)
Cardiac Index (L/min/m2)
4.0
3.5
3.0
2.5
2.0
***
***
P = 0.005
HV
CC
DC
B)
Cardiac Wall Mass Index (g/m2)
50
40
30
20
10
0
****
*
P = 0.02
HV
CC
DC
C)
Heart Rate (bpm)
90
80
70
60
50
***
****
P < 0.001
HV
CC
DC

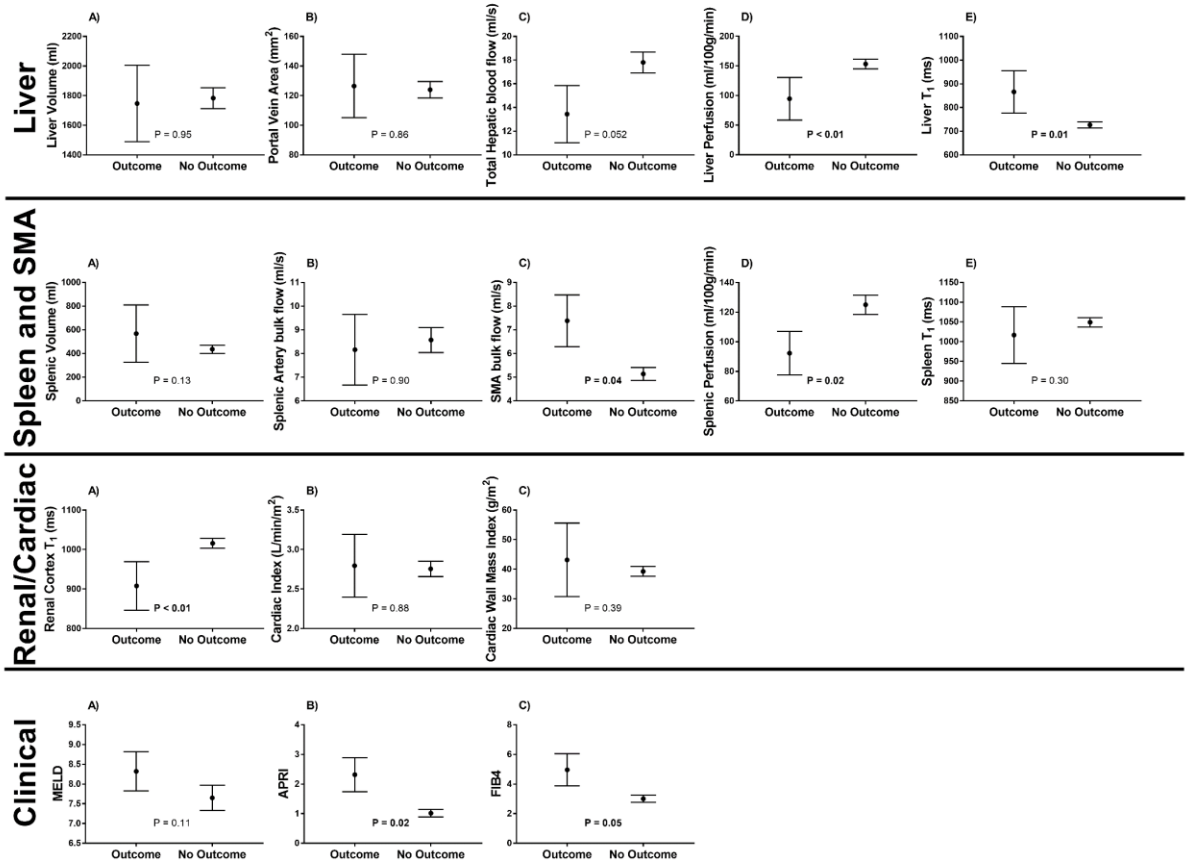
Liver
A)
Liver Volume (ml)
P = 0.95
B)
Portal Vein Area (mm²)
P = 0.86
C)
Total Hepatic blood flow (ml/s)
P = 0.052
D)
Liver Perfusion (ml/100g/min)
P < 0.01
E)
Liver T1 (ms)
P = 0.01
Outcome
No Outcome
Spleen and SMA
A)
Splenic Volume (ml)
P = 0.13
B)
Splenic Artery bulk flow (ml/s)
P = 0.90
C)
SMA bulk flow (ml/s)
P = 0.04
D)
Splenic Perfusion (ml/100g/min)
P = 0.02
E)
Spleen T1 (ms)
P = 0.30
Renal/Cardiac
A)
Renal Cortex T1 (ms)
P < 0.01
B)
Cardiac Index (L/min/m²)
P = 0.88
C)
Cardiac Wall Mass index (g/m²)
P = 0.39
Clinical
A)
MELD
P = 0.11
B)
APRI
P = 0.02
C)
FIB4
P = 0.05

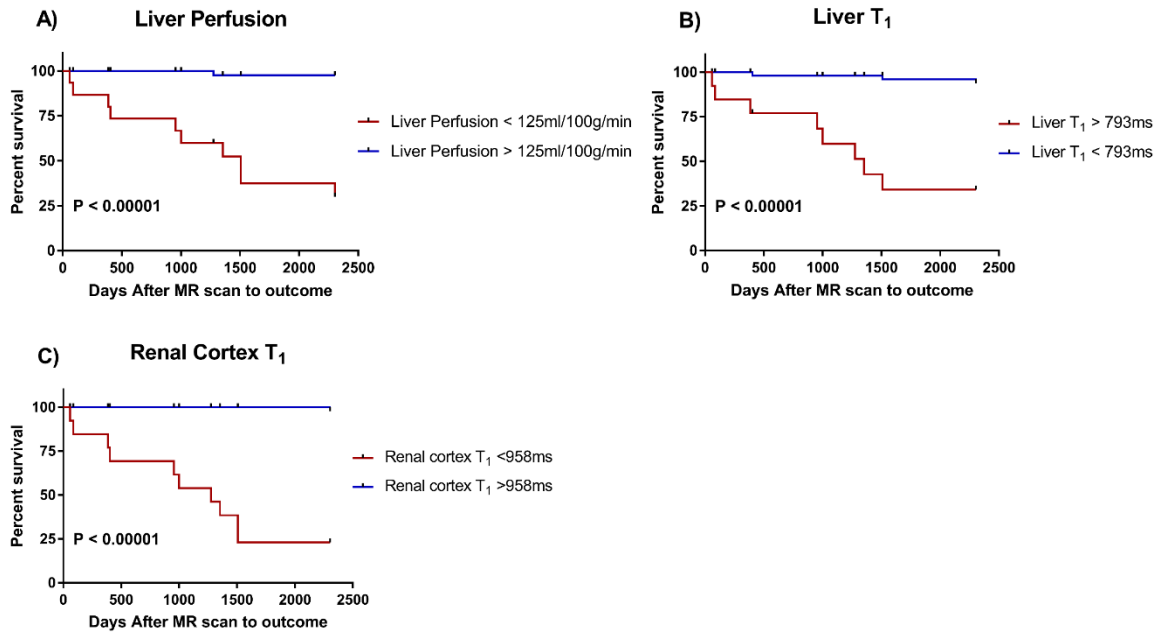
A)
Liver Perfusion
Percent survival
P < 0.00001
Days After MR scan to outcome
Liver Perfusion < 125ml/100g/min
Liver Perfusion > 125ml/100g/min
B)
Liver T1
Liver T1 > 793ms
Liver T1 < 793ms
C)
Renal Cortex T1
Renal cortex T1 <958ms
Renal cortex T1 >958ms

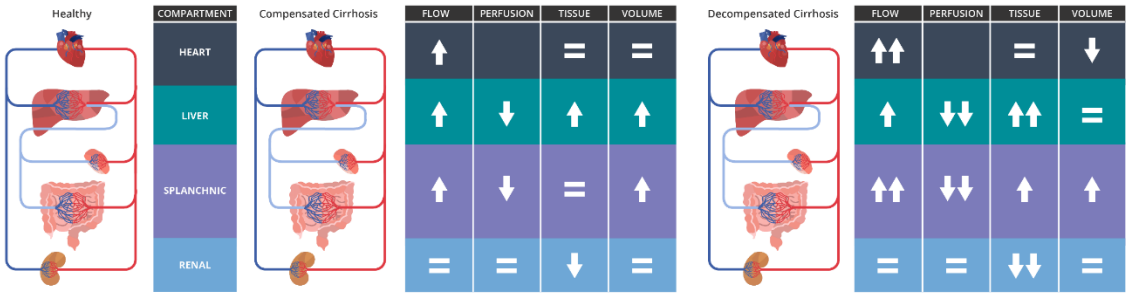
Healthy
COMPARTMENT
HEART
LIVER
SPLANCHNIC
RENAL
Compensated Cirrhosis
FLOW
PERFUSION
TISSUE
VOLUME
Decompensated Cirrhosis
FLOW
PERFUSION
TISSUE
VOLUME

Supplementary Figures and Tables

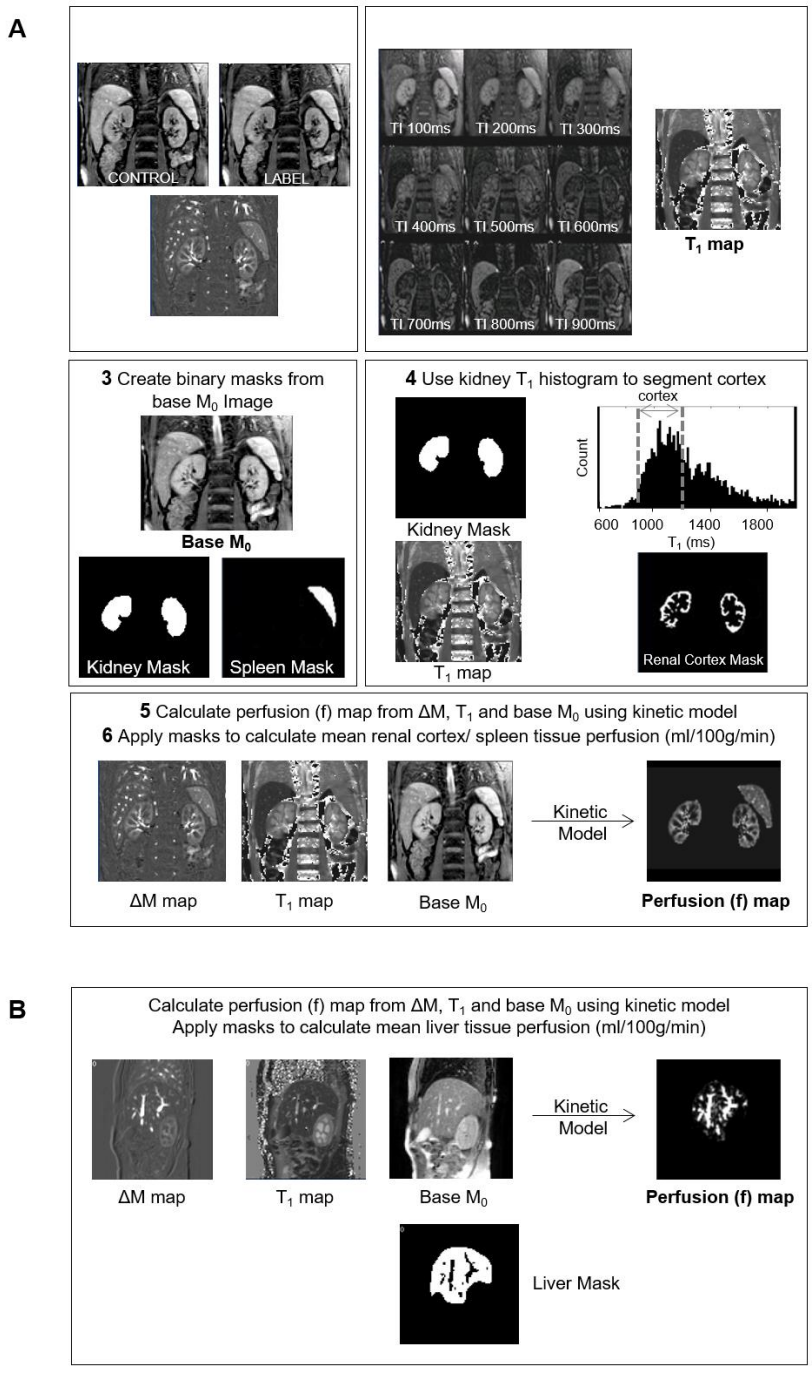

Supplementary Fig. 1. Analysis pipeline for A) renal and spleen, and B) liver T1 and ASL data. Example image analysis indicating segmentation of the kidneys, definition of cortex and medulla masks using histogram analysis, and the application of the renal cortex mask to an

arterial spin labelling perfusion map allowing the interrogation of renal cortex perfusion. Similar steps are performed to assess perfusion and T_1 values in the spleen and liver.

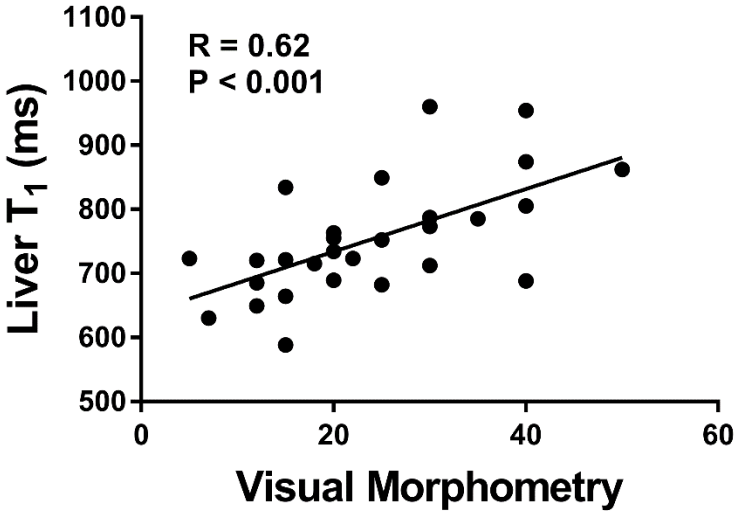

Supplementary Fig. 2. Liver T_1 relaxation time as a measure of fibrosis as assessed by gold standard liver biopsy. Scatter plot of the distribution of liver T_1 relaxation time with pathologist's estimate of fibrosis in F4 group, based on the methods described in [17]. Spearman rho and p-value of correlation shown.

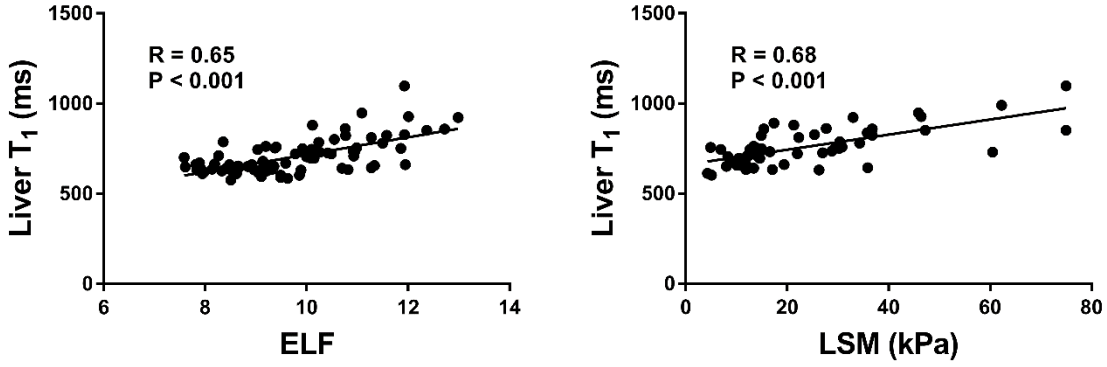

Supplementary Fig. 3. Liver T_1 relaxation time as a measure of ELF and LSM. Scatter plot of distribution of liver T_1 relaxation time with ELF and LSM as measured from Fibroscan®, with Spearman rho and p-value of correlation shown.

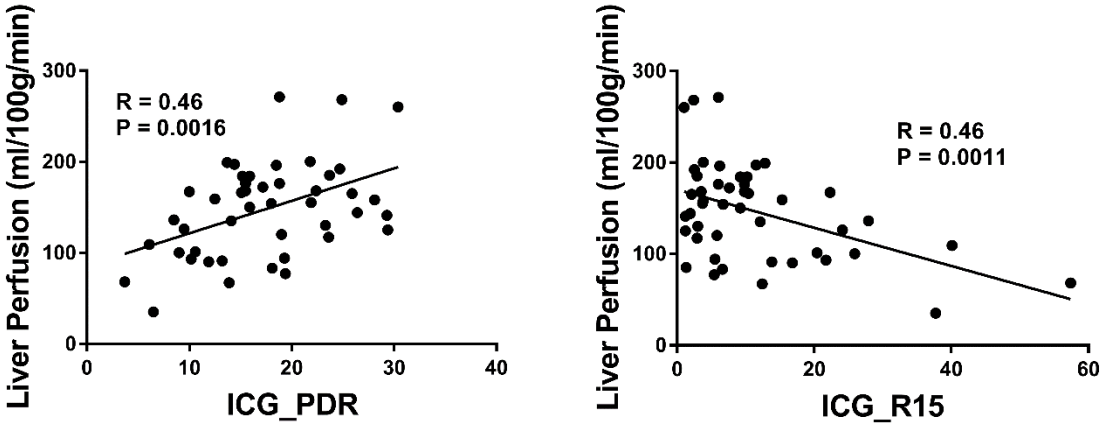

Supplementary Fig. 4. Liver perfusion as a measure of ICG-PDR and ICG_R15. Scatter plot of distribution of liver T_1 relaxation time with plasma disappearance rate (ICG-PDR) and retention rate at 15 minutes (ICGR15), with Spearman rho and p-value of correlation shown.

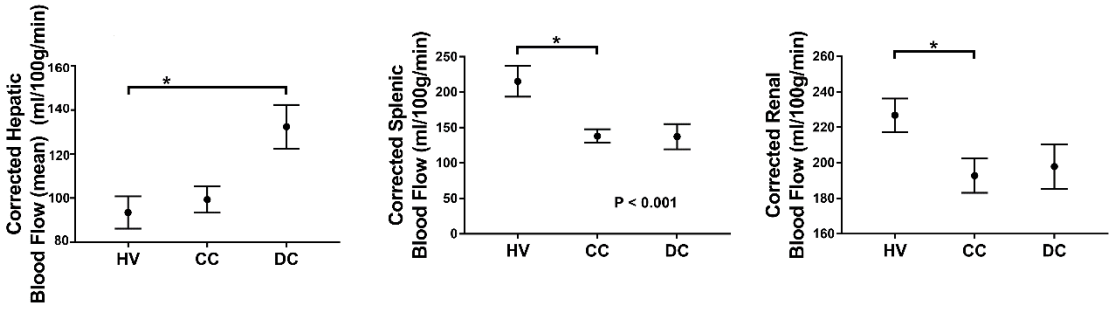

Supplementary Fig. 5. Organ volume normalised blood flow measures in healthy volunteers (HV), compensated cirrhosis patients (CC) and decompensated patients (DC). Plots shown for normalised liver blood flow, normalised splenic blood flow, and normalised renal blood flow. Data analyzed using one-way ANOVA, followed by the Tukey *post hoc* test. *$p < 0.05$, **$p < 0.01$, ***$p < 0.005$, ****$p < 0.001$.

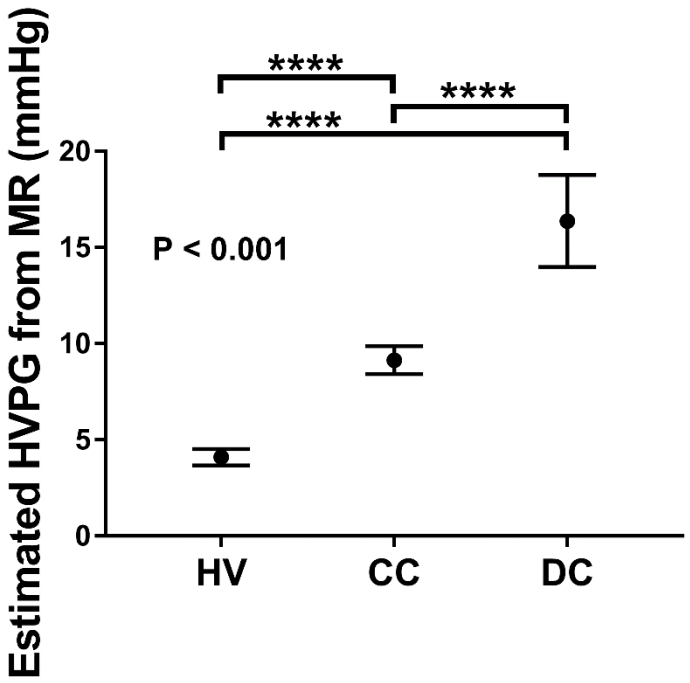

Supplementary Fig. 6. Estimated HVPG. Estimated HVPG computed using liver T_1 and splenic artery velocity measures, based on the model proposed in [20].

Supplementary Table 1: Intra-subject repeatability for the multiparametric MRI measures.

Abbreviations: CoV coefficient of variation; CSA cross sectional area; SMA superior mesenteric artery; T_1 longitudinal relaxation time.

Liver	CoV (%)	Spleen and SMA	CoV (%)	Renal/Cardiac	CoV (%)
Liver volume	4.6	Spleen volume	5.2	Renal volume	4.2
Liver T_1	1.5	Spleen T_1	1.8	Cortex T_1 Medulla T_1	2.0 1.8
Portal vein flow	18.6	Splenic artery flow	11	Renal Artery Flow	14.4
Portal vein CSA	9.5	Splenic artery CSA	7.3	Renal Artery CSA	11.1
Hepatic artery flow	22.7	SMA flow	7.6	Global single kidney perfusion	14.9
Hepatic artery CSA	13.3	SMA CSA	5.3	ASL renal cortex perfusion	9.3
ASL Perfusion	12	Spleen perfusion	6.9	Cardiac Index	8.2

Supplementary Table 2: Baseline characteristics of healthy volunteers, and the compensated and decompensated cirrhosis patients.

MR measure	Healthy volunteer	CC Patients	DC patients
Liver volume (ml)	1480 ± 63	1778 ± 61	1523 ± 111
Liver T_1 (ms)	637 ± 5	748 ± 14	864 ± 48
Portal vein flow (ml/s)	11.0 ± 0.6	12.9 ± 0.8	14.9 ± 3.0
Portal vein CSA (mm^2)	93.7 ± 3.4	124.4 ± 4.9	105.3 ± 13.9
Portal vein mean velocity (cm/s)	12.0 ± 0.6	11.0 ± 0.7	13.9 ± 2.0
Portal vein flow per beat (ml)	11.0 ± 0.6	11.9 ± 0.8	11.9 ± 2.2
Hepatic Artery flow (ml/s)	3.21 ± 0.3	4.3 ± 0.3	4.6 ± 0.9
Hepatic Artery CSA (mm^2)	23.3 ± 1.1	25.4 ± 1.1	28.2 ± 3.0
Hepatic Artery mean velocity (cm/s)	13.9 ± 1.1	17.4 ± 1.1	15.7 ± 2.9

Hepatic Artery flow per beat (ml)	3.3 ± 0.3	4.0 ± 0.3	3.7 ± 0.7
Total hepatic flow (ml/s)	14.0 ± 0.8	17.0 ± 0.9	19.2 ± 2.5
Liver perfusion (ml/100g/min)	185.1 ± 9.8	141.5 ± 7.9	100.5 ± 9.5
Splenic volume (ml)	205 ± 16	459 ± 34	489.5 ± 112
Splenic T1 (ms)	1031 ± 11	1044 ± 11	1075 ± 50
Splenic Artery flow (ml/s)	6.3 ± 0.5	8.5 ± 0.5	11.4 ± 1.5
Splenic Artery CSA (mm^2)	30.5 ± 1.6	36.4 ± 2.8	31.5 ± 3.0
Splenic artery mean velocity (cm/s)	21.6 ± 1.4	26.0 ± 1.5	38.6 ± 7.0
Splenic Artery flow per beat (ml)	6.6 ± 0.6	7.9 ± 0.5	9.1 ± 1.2
SMA flow (ml/s)	4.6 ± 0.3	5.5 ± 0.3	7.7 ± 1.1
SMA CSA (mm^2)	23.6 ± 1.2	25.3 ± 1.1	26.6 ± 2.2

SMA mean velocity (cm/s)	19.7 ± 0.7	21.7 ± 0.8	30 ± 4.7
SMA flow per beat (ml)	4.5 ± 0.2	5.0 ± 0.3	6.2 ± 0.8
Splenic perfusion (ml/100g/min)	151 ± 7	120 ± 6	81 ± 9
Renal volume (ml)	316 ± 10	336 ± 10	355 ± 28
Renal T1 (ms)	1318 ± 16	1295 ± 17	1240 ± 60
Renal Artery flow (ml/s)	5.6 ± 0.2	5.7 ± 0.2	5.6 ± 0.6
Renal Artery CSA (mm^2)	20.5 ± 0.7	21.3 ± 0.8	22.1 ± 2.2
Renal artery mean velocity (cm/s)	27.6 ± 0.8	25.9 ± 1.1	26.7 ± 4.0
Renal Artery flow per beat (ml)	5.7 ± 0.2	4.9 ± 0.2	4.5 ± 0.6
Renal cortex perfusion (ml/100g/min)	223 ± 8	215 ± 11	199 ± 26
Cardiac Index ($L/min/m^2$)	2.42 ± 0.06	2.76 ± 0.09	3.06 ± 0.38

Cardiac Wall mass Index (g/m^2)	39.0 ± 1.1	40.0 ± 1.7	22.3 ± 2.4
Heart rate	59.6 ± 1.6	67.2 ± 1.6	76.2 ± 3.1

Supplementary Table 3: Characteristsics of the compensated cirrhosis patients with and without liver related outcome (LRO). All values shown are mean (standard deviation) except * which indicates median and interquartile range.

MR measure	LRO	No LRO	P value
Liver volume (ml)	1948 (521)	*1728 (740)	0.25
Liver T_1 (ms)	853.7 (125)	720 (73)	<0.001
Portal vein flow (ml/s)	8.7 (6.5)	13.8 (5.7)	0.01
Hepatic Artery flow (ml/s)	3.8 (1.9)	4.1 (2.7)	0.58
Total hepatic flow (ml/s)			
Liver perfusion (ml/100g/min)	93.3 (32.2)	162.5 (46.2)	<0.001
Splenic volume (ml)	550 (331)	432 (224)	0.14
Splenic T1 (ms)	1001 (80)	1048 (74)	0.09
Splenic Artery flow (ml/s)	8.2 (3.3)	8.6 (3.3)	0.79
SMA flow (ml/s)	7.4 (3.6)	*4.6 (2.8)	0.04
Splenic perfusion (ml/100g/min)	92.3 (41.8)	125.1 (39.4)	0.04
Renal volume (ml)	348 (82)	340 (67)	0.76

Renal T1 (ms)			
Cortex	909 (89)	1012 (71)	<0.001
Medulla	1149 (119)	1321 (97)	<0.001
Cortoicomedullary difference	239 (44)	292 (80)	0.003
Renal Artery flow (ml/s)	5.74 (1.8)	5.38 (1.8)	0.56
Renal cortex perfusion (ml/100g/min)	234 (109)	211 (60)	0.437
Cardiac Index (L/min/m^2)	2.8 (0.6)	*2.7(0.7)	0.77
Cardiac Wall mass Index (g/m^2)	41.9 (16.2)	39.8 (11.8)	0.86